MIMO Self-Heterodyne OFDM

Nirmal Fernando, Yi Hong, *Senior Member, IEEE*, and Emanuele Viterbo, *Fellow, IEEE*

***Abstract*—Self-heterodyne orthogonal frequency-division multiplexing (self-het OFDM) is a promising physical-layer technique for millimeter-wave and terahertz RF communication due to its simple RF front end and complete immunity against frequency offset and phase noise. In this paper, we proposed a multiple-input–multiple-output (MIMO) self-het OFDM with the adaption of the smart carrier positioning (SCP) technique. At the transmitter, a space–time block code (STBC) is used to produce the coded information symbols to be transmitted on each antenna over the self-het OFDM subcarriers. At the receiver, a simple nonlinear detection is adopted at each receive antenna. The achievable diversity order of such setting is analyzed, and it is found that with the adaptation of the SCP technique, the diversity loss in comparison to the conventional coherent MIMO-OFDM can be compensated. We further derive analytically both lower and upper bounds on the diversity order of the proposed scheme, and simulations will be shown to illustrate the performance of such combination.**

***Index Terms*—Alamouti code, direct detection (DD), Golden code, millimeter wave, multiple-input multiple-output (MIMO), noncoherent detection, orthogonal frequency-division multiplexing (OFDM), self-heterodyne (self-het), terahertz RF.**

I. Introduction

HIGH-SPEED indoor multimedia networking has driven a growing research interest in millimeter-wave and terahertz RF communications due to the availability of large chunks of free spectrum. However, coherent demodulation front-end components, such as carrier phase recovery phase-locked loop circuits and oscillators, are complex and highly sensitive [1], [2]. In particular, these RF components generate high phase noise at the receiver, and advanced frequency stabilization techniques are needed to control it at the expense of high receiver complexity [3].

An alternative approach is to use direct detection (DD) techniques, based on zero-bias (ZB) Schottky barrier diodes [4] and micromachined millimeter-wave integrated circuits (MMICs) [5], [6]. These devices are equipped with near-ideal "square-law" characteristics, where the output electrical signal is directly proportional to the squared received RF signal magnitude. Moreover, these semiconductor devices have excellent phase noise performance and can replace complex frequency stabilization techniques at the receiver.

The self-heterodyne (self-het) downconversion technique [3] together with the DD technique can provide simple and stable RF receivers for millimeter-wave and terahertz RF frequencies. Self-het downconversion was originally proposed to combat phase noise in 60-GHz RF bands. Later, in [7], it was shown experimentally that this technique can be used in conjunction with orthogonal frequency-division multiplexing (OFDM; i.e., self-het OFDM), where the sensitivity to phase noise is critical in choosing the subcarrier spacing. In self-het OFDM, the transmitter jointly sends the RF carrier and the OFDM subcarriers separated by a guard band. The insertion of the guard band reduces the bandwidth efficiency of self-het OFDM by 50% [18]. At the receiver, a self-mixing square-law device (e.g., ZB Schottky diode detector circuit) is used to downconvert the RF signal without the need of a local carrier, carrier phase recovery, and carrier frequency correction. The role of the guard band is to avoid self-mixing interference produced by the nonlinear device. Since the transmitter can ensure that the local carrier phase is synchronized with the OFDM subcarriers, the self-het OFDM downconversion is simple, stable, and immune to phase noise. In [8], it was experimentally demonstrated that MMICs with multiple passive detectors can significantly increase the receiver sensitivity. Since then, there has been a number of recent research developments on self-het OFDM, as shown in [9]–[13].

Early study on channel characteristics of millimeter-wave RF channels suggests that these channels can be frequency selective in both line-of-sight (LOS) and non-LOS conditions [14], [15]. This is mainly due to the reflective nature of millimetre-wave RF signals [16], [17]. In [18], we analyze self-het OFDM for a single-input–single-output (SISO) frequency-selective channel. A pairing scheme is then presented in [19] to exploit the unbalance in signal-to-interference-plus-noise ratios (SINRs) naturally occurring in the subcarriers of a self-het OFDM.

In this paper, we extend our previous study on SISO self-het OFDM [18] to a MIMO setting. For MIMO millimeter-wave communications, it was suggested in [20] and [21] that directional antennas are needed to compensate for the path loss and enhance receive power for such small wavelengths. Such a setting results in a sparse multipath channel. It was also pointed out in [20] and [21] that it is possible to obtain a high-rank MIMO channel by using multiple antennas spaced several wavelengths apart. On one hand, to combat multipath effects, conventional OFDM techniques can be used, where each subcarrier is assumed to experience an independent fading that can be modeled as independent and identically distributed (i.i.d.) complex Gaussian random variables. On the other hand, better performance of MIMO millimeter-wave communications can

Manuscript received June 4, 2014; revised September 3, 2014, October 20, 2014, and January 26, 2015; accepted March 5, 2015. Date of publication March 9, 2015; date of current version March 10, 2016. This work was supported by the Australian Research Council Discovery Project under Grant ARC DP130100336. The review of this paper was coordinated by Dr. N.-D. Đào.

N. Fernando was with Monash University, Clayton, Vic. 3800, Australia. He is now with Airservices Australian, Brisbane, Qld. 4009, Australia (e-mail: nirmal.chathura@gmail.com).

Y. Hong and E. Viterbo are with the Department of Electrical and Computer System Engineering, Monash University, Clayton, Vic. 3800, Australia (e-mail: Yi.Hong@monash.edu; Emanuele.Viterbo@monash.edu).

Color versions of one or more of the figures in this paper are available online at http://ieeexplore.ieee.org.

Digital Object Identifier 10.1109/TVT.2015.2411277

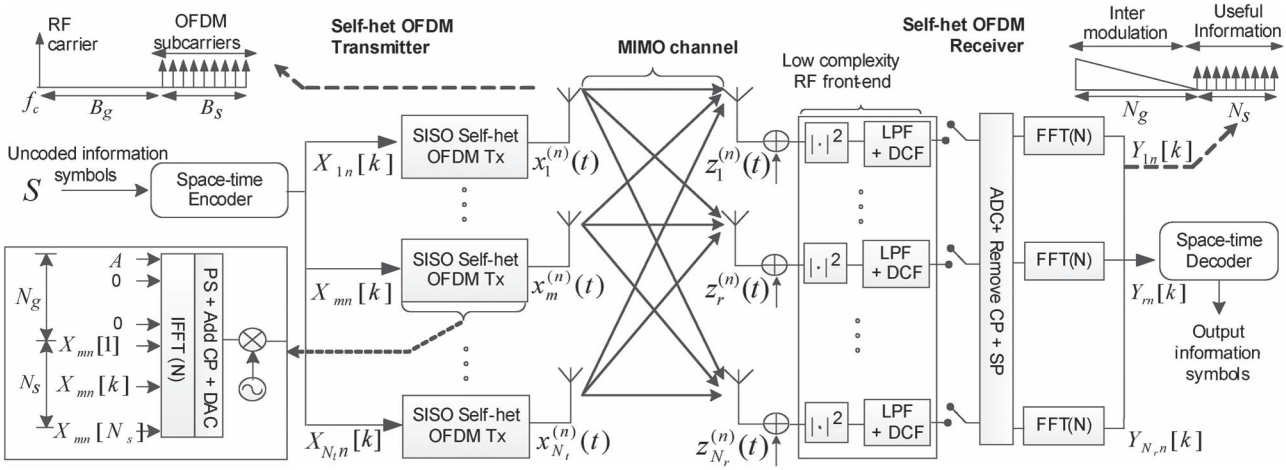

Fig. 1. MIMO self-het OFDM.

be obtained by using space–time coding technique, as demonstrated in [20]. In this paper, we consider a space–time block coded (STBC) MIMO self-het OFDM[1] to achieve good performance by mitigating multipath effects and high-level oscillator instabilities with an extremely low complexity RF front end. The specific contributions of our paper are given next.

- We consider the well-known the Alamouti code [23] and the Golden code [25], respectively, as the STBC schemes. As an approximate measure of quality, we analyze the diversity order of STBC MIMO self-het OFDM and find that there is a diversity loss when compared with the traditional STBC MIMO-OFDM. This is due to the use of a common RF carrier from each transmit antenna in MIMO self-het OFDM. Specifically, the STBC MIMO self-het OFDM experiences a doubly faded channel, where one fade is due to multipath and the other is incurred by the RF carrier in each link between transmitter/receiver antenna pairs.
- To compensate this loss, we modify the *smart carrier positioning* (SCP) technique, which was originally proposed in [18] for the SISO case. In the SISO case, the carrier was positioned in an OFDM subchannel with the highest gain to improve the bit error rate (BER) of the system. In the MIMO case, a common carrier is placed in a subcarrier position that jointly maximizes the overall MIMO channel gain and optimizes the diversity order. Under such a setting, we analyze the achievable diversity gain of the proposed SCP scheme. We first derive both upper and lower bounds on the diversity gain. We then show analytically and by simulation that the SCP STBC MIMO self-het OFDM can increase the diversity gain.

This paper is organized as follows. In Section II, we introduce the system model for MIMO self-het OFDM. In Section III, we consider two STBCs (Alamouti and Golden codes) for MIMO self-het OFDM, and we prove that there is a diversity loss in such a system. In Section IV, we present the SCP technique to compensate this diversity loss, and we theoretically prove that SCP can improve diversity order by at least one. In Section V, we show the simulation results. Finally, we draw conclusions in Section VI.

Throughout this paper, we adopt the following notation: $\Re\{\cdot\}$ denotes the real component of a complex number, j denotes the imaginary unit, $*$ represents the convolution operation, $|a|$ represents the absolute value of a, A^H represents the Hermitian matrix of A, $\mathbb{C}^{M\times N}$ represents an $M \times N$ complex matrix, $E[x]$ represents the expectation of a random variable x, $f_X(x)$ denotes the probability distribution function of random variable X, $\mathfrak{L}(x)$ represents the Laplace transform of x, $K_v(\cdot)$ denotes the vth order of the modified Bessel function of second kind, $\mathbb{E}\mathrm{i}(x)$ is the exponential integral and defined by

$$\mathbb{E}i(z) \triangleq -\int_z^\infty \exp(-t)/t\, dt$$

and $Q(x)$ is the Gaussian tail function, which is defined by

$$Q(x) \triangleq \frac{1}{2\pi}\int_x^\infty \exp(-u^2/2)\, du.$$

II. System Model

A. MIMO Self-Het OFDM

A block diagram of a typical MIMO self-het OFDM communications system is shown in Fig. 1, where $\mathbf{H}$ is the MIMO channel frequency responses matrix, N_t is the number of transmit antennas, N_r is the number of receive antennas, f_c is RF carrier frequency, Δf is OFDM subcarrier spacing, N_s is the number of OFDM subcarriers used to encode information at each transmit antenna, N_g is the number of subcarriers omitted in each self-het OFDM transmitter, N $(N = N_g + N_s)$ is the size of inverse fast Fourier transform (IFFT)/fast Fourier transform (FFT), B_g is the frequency gap between the RF carrier and the first OFDM subcarrier, and B_s is the useful OFDM subcarrier bandwidth.

At the transmitter, the information is encoded by a space–time encoder to generate the codeword matrix. Let

[1]This is also known as space–frequency block coded MIMO, which is performed across OFDM tones to obtain MIMO space and frequency diversity [22].

$\mathbf{X}[k] \triangleq \{X_{mn}[k]\} \in \mathbb{C}^{N_t \times T}$ be the codeword matrix transmitted using N_t transmit antennas in the kth OFDM subcarrier over T channel uses, where $m = 1, \ldots, N_t$, $n = 1, \ldots, T$, and $k = 1, \ldots, N_s$. This coded symbol matrix is then fed column by column into N_t parallel self-het OFDM transmitters that use only the last N_s OFDM subcarriers for the transmission, whereas the remaining N_g OFDM subcarriers are set to zero (see Fig. 1). In each self-het OFDM transmitter by using an IFFT, the discrete time-domain OFDM symbol is generated as

$$s_m^{(n)}(t) = \Re\left\{\sum_{k=1}^{N_s} X_{mn}[k] e^{j2\pi(B_g + k\Delta f)t}\right\} \tag{1}$$

where $B_g = N_g \Delta f$. The parallel-to-serial (PS) conversion, the addition of cyclic prefix (CP), and the digital-to-analog conversion (DAC) are performed to generate the continuous time-domain OFDM symbol. Then, the RF signal $x_m^{(n)}(t)$ is generated by adding an RF carrier signal to $s_m^{(n)}(t)$ with a frequency gap B_g between the carrier and the first OFDM subcarrier,[2] i.e.,

$$x_m^{(n)}(t) = \left[A + s_m^{(n)}(t)\right] \cos(2\pi f_c t). \tag{2}$$

The upconverted OFDM symbols $x_m^{(n)}(t)$ are then transmitted over a MIMO channel using N_t transmit antennas. Let $w_r^{(n)}(t)$, $h_{rm}^{(n)}(t)$, and $z_r^{(n)}(t)$ be the received signal at the rth receive antenna ($r = 1, \ldots, N_r$), the channel impulse response from the mth transmitter to the rth receive antenna, and the noise component at the rth receive antenna, respectively. Then, $w_r^{(n)}(t)$ can be written as

$$w_r^{(n)}(t) = h_{rm}^{(n)}(t) * x_m^{(n)}(t) + z_r^{(n)}(t). \tag{3}$$

We assume that the zero-mean white Gaussian noise $z_r^{(n)}(t)$ with variance σ^2 is added before the nonlinear downconversion, and it is additive white Gaussian noise, i.e., $(z_r^{(n)}(t) \sim \mathcal{N}(0, \sigma^2))$, where σ^2 denotes the noise power.

At the receiver, signal detection is performed using a nonlinear device at each receiver, producing the output $|w_r^{(n)}(t)|^2$, to downconvert the passband signal to the baseband signal. Since the local carrier signal is embedded in the received signal, the above downconversion does not require any local carrier generation, carrier phase recovery, and carrier frequency correction [18]. This downconversion is more stable and simpler than that of conventional superheterodyne downconversion [3]. The downconverted signals are then passed through low-pass filters (LPFs), with a cutoff frequency $B_g + B_s$, and dc filters (DCFs) to remove the high-frequency signals and the residual dc components generated during the nonlinear downconversion. After the analog-to-digital conversion (ADC), the CP is removed, serial-to-parallel (SP) conversion is performed, and FFT recovers the transmitted symbols. As shown in [18], the condition $B_g \geq B_s$ is required to restrict the dominant intermodulation product, which is generated by the nonlinear downconversion, occurring in the first N_g OFDM subcarriers. Hence, the first N_g OFDM subcarriers are ignored since they contain only the intermodulation products, as shown in Fig. 1. The next N_s OFDM subcarriers that contain the transmitted symbols are forwarded to the space–time decoder to extract the transmitted information.

[2]This can equivalently be realized by inserting in the first OFDM subcarrier, i.e., a dc component A, as shown in Fig. 1.

The discrete equivalent baseband model for a SISO channel, which was given in [18], can be extended to the MIMO case. For simplicity, in the following, we drop the index k since we only consider one OFDM subcarrier at a time. For an arbitrary OFDM subcarrier, we have

$$\mathbf{Y} = \mathbf{H}_\mathbf{c}^* \mathbf{H}\mathbf{X} + \hat{\mathbf{Z}} \tag{4}$$

where $\mathbf{Y} \triangleq \{Y_{rn}\} \in \mathbb{C}^{N_r \times T}$, $\mathbf{H} \triangleq \{H_{rm}\} \in \mathbb{C}^{N_r \times N_t}$, and $\hat{\mathbf{Z}} \triangleq \{\hat{Z}_{rn}\} \in \mathbb{C}^{N_r \times T}$ represent the received symbol matrix, the frequency response of the MIMO channel, and the equivalent noise/interference component after the nonlinear downconversion, respectively. In (4), the diagonal matrix $\mathbf{H}_c \triangleq \text{diag}\{\sum_{m=1}^{N_t} H_{rm}^{(c)}\}$ with $H_{rm}^{(c)}$ represents the channel frequency response evaluated at the carrier frequency from the mth transmit antenna to the rth receive antenna. In moderate and high SNR regions, from [18, Sec. III-B, eq. (17)] , the noise variance for the subcarrier k at receiver r averaged over the channel realization $\mathbf{H}$, but conditioned on the carrier frequency response $\mathbf{H}_c$, is approximately given by

$$\sigma_{\hat{Z}_r}^2 \cong \sigma^2 \left(\left| \sum_{r=1}^{N_r} H_{rm}^{(c)} \right|^2 + \frac{\lambda_r(k)}{\eta N_s} \right) \tag{5}$$

where η denotes the RF carrier-to-signal power ratio [18], $k = 1, \ldots, N_s$, $r = 1, \ldots, N_r$, and

$$\lambda_r(k) \cong \sigma^2 \frac{2(N_s - k)}{(N_g + N_s)} \mathbf{E}\left[\sum_{k=1}^{N_s} \sum_{m=1}^{N_t} |H_{rm}^{(k)}|^2 \right]. \tag{6}$$

Since

$$\mathbf{E}\left[\sum_{k=1}^{N_s} \sum_{m=1}^{N_t} |H_{rm}^{(k)}|^2 \right] = N_s N_t \tag{7}$$

and we assume $N_g = N_s$, we have

$$\sigma_{\hat{Z}_r}^2 = \sigma^2 \left(\left| \sum_{r=1}^{N_r} H_{rm}^{(c)} \right|^2 + \frac{N_t}{\eta N_s} (N_s - k) \right). \tag{8}$$

This shows that every subcarrier has a different SINR.

III. Space-Time Block Code Multiple-Input–Multiple-Output Self-Het Orthogonal Frequency Division Multiplexing

Here, we will consider two types of STBC codes for 2×2 MIMO self-het OFDM: 1) the Alamouti code [23] and 2) the Golden code [25]. For simplicity, we still drop the OFDM subcarrier index $k = 1, \ldots, N_s$. It was pointed out in [20] and [21] that by using multiple directional antennas spaced several wavelengths apart, the MIMO channels can be assumed to be independent. Since the multipath component channels can be equalized by the OFDM technique, we assume that the channel response coefficients for each subcarrier are i.i.d. complex

Gaussian with zero mean and unit variance (also known as Rayleigh fading), i.e., $H_{rm}^{(c)}, H_{rm} \sim \mathcal{N}(0,1)$, where $r = 1, 2$ and $m = 1, 2$.

A. Alamouti Code [23]

Let $\mathbf{S} = [S_1, S_2]^T$ be the uncoded M-ary quadrature-amplitude modulation (M-QAM) information symbol vector to be transmitted over two consecutive OFDM symbols in the kth OFDM subcarrier, and the energy of each symbol is denoted by E_s. The Alamouti encoder generates the following codeword matrix [23]:

$$\mathbf{X} = \begin{bmatrix} S_1 & -S_2^* \\ S_2 & S_1^*. \end{bmatrix} \tag{9}$$

Let $\alpha_c \triangleq H_{11}^{(c)} + H_{12}^{(c)}$ and $\beta_c \triangleq H_{21}^{(c)} + H_{22}^{(c)}$. Using Alamouti preprocessing [23] and from (4), we have

$$\underbrace{\begin{bmatrix} Y_{11} \\ Y_{21} \\ Y_{12}^* \\ Y_{22}^* \end{bmatrix}}_{\triangleq \hat{\mathbf{Y}}} = \underbrace{\begin{bmatrix} \alpha_c^* H_{11} & \alpha_c^* H_{12} \\ \beta_c^* H_{21} & \beta_c^* H_{22} \\ \alpha_c H_{12}^* & -\alpha_c H_{11}^* \\ \beta_c H_{22}^* & -\beta_c H_{21}^* \end{bmatrix}}_{\triangleq \mathbf{H}_{\text{eq}}} \begin{bmatrix} S_1 \\ S_2 \end{bmatrix} + \underbrace{\begin{bmatrix} \hat{Z}_{11} \\ \hat{Z}_{21} \\ \hat{Z}_{12}^* \\ \hat{Z}_{22}^* \end{bmatrix}}_{\triangleq \hat{\mathbf{Z}}}. \tag{10}$$

Let $\mathbf{H}_{\text{eq}}^{\dagger}$ be the pseudoinverse of $\mathbf{H}_{\text{eq}}$, and

$$\mathbf{H}_{\text{eq}}^{\dagger} \triangleq \left(\mathbf{H}_{\text{eq}} \mathbf{H}_{\text{eq}}^H\right)^{-1} \mathbf{H}_{\text{eq}}^H = \frac{1}{\Lambda} \mathbf{H}_{\text{eq}}^H \tag{11}$$

where

$$\Lambda \triangleq \underbrace{|\alpha_c|^2 \left(\sum_{m=1}^{2} |H_{1m}|^2 \right)}_{\triangleq \Lambda_1} + \underbrace{|\beta_c|^2 \left(\sum_{m=1}^{2} |H_{2m}|^2 \right)}_{\triangleq \Lambda_2}. \tag{12}$$

At the receiver, a zero-forcing equalizer or maximum-likelihood detection (MLD) can be used to recover the information symbols by considering the $\mathbf{H}_{\text{eq}}^{\dagger} \hat{\mathbf{Y}}$ vector.

It is known that conventional MIMO-OFDM schemes using the Alamouti code achieves diversity order of 4 in 2×2 MIMO systems [24]. However, in the following, we prove that MIMO self-het OFDM using the Alamouti code only provides diversity 2.

Proposition 1: The achievable diversity order of 2×2 Alamouti-coded MIMO self-het OFDM is 2 for MIMO channels.

Proof: See Appendix A. ■

We note that this diversity loss is due to the fact that the use of RF carrier undergoes independent fading from the same OFDM subchannel of the two incoming links at each receive antenna. Specifically, we can observe that the channel matrix in (10) is different from that of conventional Alamouti-coded MIMO-OFDM schemes, where $\alpha_c = 1$ and $\beta_c = 1$. From (12), we observe that the carrier fading terms multiply the standard MIMO channel fading terms, resulting in a doubly faded channel, as we will analyze in the following section.

B. Golden Code [25]

The Golden code is an optimal full-rate full-diversity STBC code for a coherent 2×2 MIMO channel, which has nonvanishing determinant property [25] and achieves the diversity–multiplexing frontier [26]. Let $\mathbf{S} = [S_1, S_2, S_3, S_4]^T$ be the uncoded M-QAM information symbol vector to be transmitted over two consecutive OFDM symbols in the kth OFDM subcarrier. The algebraic construction yields codewords of the Golden code of the form [25]

$$\mathbf{X} = \frac{1}{5} \begin{bmatrix} \alpha(S_1 + \theta S_2) & \alpha(S_3 + \theta S_4) \\ j\sigma(\alpha)(S_3 + \sigma(\theta) S_4) & \sigma(\alpha)(S_1 + \sigma(\theta) S_2) \end{bmatrix} \tag{13}$$

where $\theta = (1 + \sqrt{5})/2$, $\sigma(\theta) = 1 - \theta$, $\alpha = 1 + j\sigma(\theta)$, and $\sigma(\alpha) = 1 + j\theta$. Let $\mathbf{G}$ be the generator matrix for the Golden code, i.e., $\mathbf{X} = \mathbf{GS}$, and the $\mathbf{G}$ matrix is given in [25]. At the receiver, MLD is performed to decode the original information symbols as

$$\hat{\mathbf{S}} = \arg\min_{S} \; \|\mathbf{Y} - \mathbf{H}_{\mathbf{c}}^* \mathbf{H} \mathbf{G} \mathbf{S}\|^2 \tag{14}$$

where $\hat{\mathbf{S}}$ is the estimated received symbol vector in the kth OFDM subcarrier. Since the complexity of MLD exponentially grows with higher order signal constellations, sphere-decoder-based MLD [27] can be used to achieve the best performance with reduced decoding complexity.

We remark that fast decodable STBC codes, e.g., silver code [29], [30], can be also implemented in MIMO, similarly to the Golden code.

IV. Self-Het Multiple-Input–Multiple-Output Enhancements

A. SCP Technique

In *Proposition 1*, we show that STBC-encoded MIMO self-het OFDM cannot exploit the full diversity gain. More specifically, it was shown in Appendix A that the diversity order of a communication system is directly related to the instantaneous SINR (γ) distribution of the OFDM subcarriers. The distribution of γ is determined by the behavior around zero of the distribution of the random variable Λ defined in (12). Hence, the diversity order of Alamouti-coded MIMO self-het OFDM systems can be improved by optimizing the distribution of Λ. We therefore consider the SCP technique originally proposed in [18] for the SISO case. Different from the SISO case, where the carrier was positioned in an OFDM subchannel with the highest gain, in the MIMO case, the carrier will be placed in a subcarrier that jointly maximizes the MIMO channel gain and optimizes the diversity order, which is a standard measure of the performance of STBC [23], [28], [30]. The details on the proposed SCP for MIMO self-het OFDM is given in the following discussion.

At the transmitter, the SCP places the RF carrier in either the lower band or the upper band with respect to the OFDM subcarriers [see Fig. 2(a) and (b)]. If the RF carrier is placed in the higher band, the information subcarriers can be transmitted in the lower band, and the transmitted OFDM symbols are $X_{mn}^*[k]$, instead of $X_{mn}[k]$. After the nonlinear detection, both subcarrier placements give the same result.

Let P be the total number of possible carrier positions (equally spaced by Δf), where $l \in \{1, \ldots, P/2, N - P/2 - 1,$

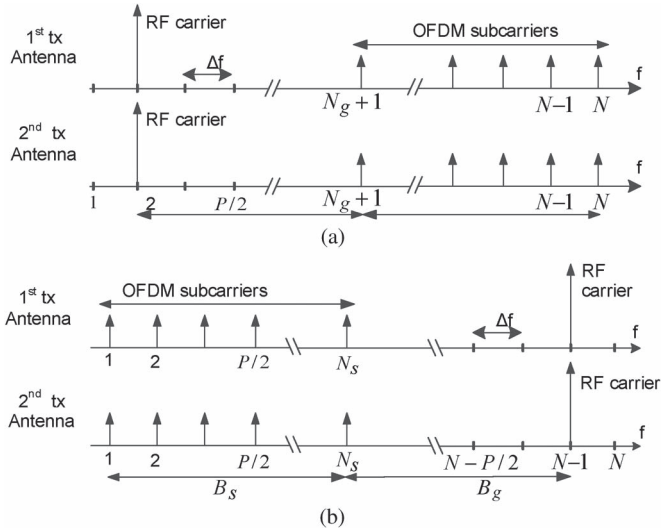

Fig. 2. SCP technique in STBC-encoded MIMO self-het OFDM. (a) RF carrier transmitting in the lower band. (b) RF carrier transmitting in the upper band.

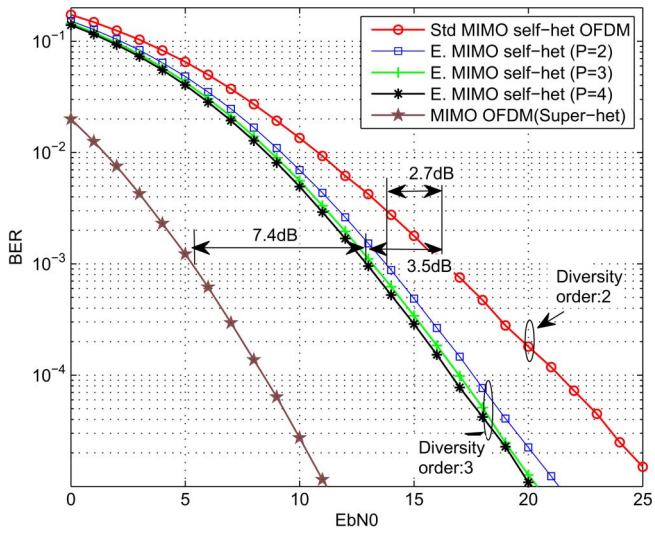

Fig. 3. BER performance of 2×2 MIMO self-het OFDM using the Alamouti code and the SCP technique (no phase noise).

$\ldots, N\}$ is the RF carrier position. Let us define

$$\alpha_c^{(l)} \triangleq H_{11}^{(l)} + H_{12}^{(l)} \text{ and } \beta_c^{(l)} \triangleq H_{21}^{(l)} + H_{22}^{(l)} \tag{15}$$

where $H_{rm}^{(l)}$ is the channel frequency response from the mth transmit antenna to the rth receive antenna at the lth potential RF carrier position. If the channel length is considerably larger than the OFDM symbol duration, for a given OFDM symbol transmission, we assume that H_{rm} for $r, m = 1, 2$ are independent random variables from $\alpha_c^{(l)}$ and $\beta_c^{(l)}$. Since $E[|H_{rm}|^2] = 1$, where $r, m = 1, 2$, the expectation of Λ over k can be approximated as

$$E[\Lambda] \approx 2\left(\left|\alpha_c^{(l)}\right|^2 + \left|\beta_c^{(l)}\right|^2\right)$$

for a given lth RF carrier position. As shown in Fig. 2, if the MIMO channel is known, we can select the optimum carrier position by

$$l^* = \underset{\substack{l \in \left\{1,\ldots \frac{P}{2}, \\ N-\frac{P}{2},\ldots,N\right\}}}{\arg\max} \left\{\left(\left|\alpha_c^{(l)}\right|^2 + \left|\beta_c^{(l)}\right|^2\right)\right\} \tag{16}$$

where l^* denotes the optimum carrier position. For a general STBC MIMO-self-het OFDM, this optimization given in (16) can be extended as

$$l^* = \underset{\substack{l \in \left\{1,\ldots \frac{P}{2}, \\ N-\frac{P}{2},\ldots,N\right\}}}{\arg\max} \left\{\sum_{r=1}^{N_r}\left|\sum_{m=1}^{N_t} H_{rm}^{(l)}\right|^2\right\}. \tag{17}$$

After choosing the best l^* in (16), we let $p = l^*$, if the carrier is positioned on the left-hand side, or $p = N + 1 - l^*$, if on the right-hand side. Then, we have $B_g = B_s = \Delta f(N + 1 - p)/2$, where $p \in \{1, 2, 3, \ldots, P/2\}$. We will show in Section V that the SCP technique for the MIMO case requires very limited number of feedback information, i.e., a few information bits to encode the index l^*.

B. Diversity Order of SCP STBC MIMO Self-Het OFDM

The diversity order of an STBC measures the reliability of the $N_t \times N_r$ MIMO communication system. We say the STBC has full diversity when the order is equal to $N_t \cdot N_r$. Here, we analyze the diversity order of 2×2 Alamouti-coded MIMO self-het OFDM using SCP ($P = 2$) over MIMO channels, and we have the following propositions.

Proposition 2: The lower bound on the diversity order of 2×2 Alamouti-coded MIMO self-het OFDM using SCP is 3.

Proof: See Appendix B. ■

Proposition 3: The upper bound on the diversity order of 2×2 Alamouti-coded MIMO self-het OFDM using SCP is 4.

Proof: See Appendix C. ■

We conclude that the actual diversity order of MIMO self-het OFDM is between 3 and 4. Due to the doubly fading effects, the order is not necessarily an integer value.

V. Simulation Results

Here, we simulate the BER performance of 2×2 MIMO self-het OFDM. We adopt the following simulation parameters: $N = 256$, $N_s = N_g = 128$, $\eta = 0.6$, sampling time $T_s = 1\ \mu$s, the maximum channel delay 64 T_s, the length of CP of $(64 + 1)T_s$, and QPSK signaling. With QPSK signaling, since half of OFDM subcarriers are unused in self-het OFDM, the spectral efficiency of self-het OFDM is 50% of that achieved by the conventional OFDM scheme using the superheterodyne structure. For comparison, we use BPSK signaling in conventional MIMO OFDM to have the same spectral efficiency.

Fig. 3 compares the BER performance of standard MIMO self-het OFDM and enhanced MIMO self-het OFDM using the SCP technique. Both systems are encoded with an Alamouti code. In this simulation, we assume no phase noise at the receiver. In contrast to standard MIMO self-het OFDM, the enhanced scheme provides approximately 2.7 and 3.5 dB gains at BER of 10^{-3} with $P = 2$ and $P = 4$, respectively. For $P \ll N$, the SCP technique consumes a negligible amount of extra

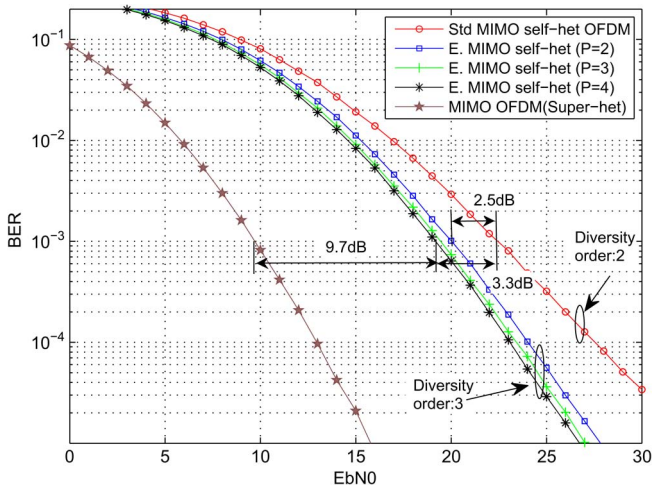

Fig. 4. BER performance of 2×2 MIMO self-het OFDM using the Golden code and the SCP technique (no phase noise).

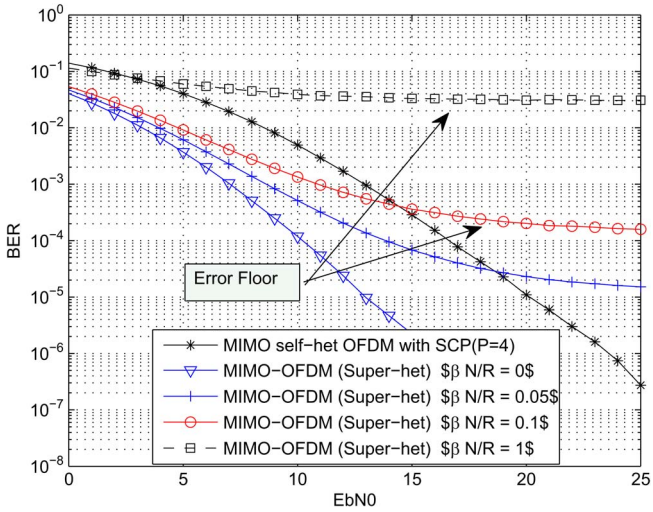

Fig. 5. BER performance comparison of Alamouti-coded MIMO self-het OFDM with SCP ($P = 4$) and Alamouti-coded MIMO-OFDM with superheterodyne in the presence of phase noise ($R = 2.133 \times 10^7$).

bandwidth. We also observe that $P = 4$ is a good compromise, since the gain saturates for $P > 4$, and the rate loss at $P = 4$ is negligible. As shown in Proposition 1, the diversity order of standard Alamouti-coded MIMO self-het OFDM is 2, which is half of that in a conventional Alamouti-coded MIMO-OFDM. As discussed in Propositions 2 and 3, the diversity order of enhanced MIMO self-het OFDM using the Alamouti code is between 3 and 4. In Fig. 3, the simulation results agree with this analytical result. Furthermore, compared with Alamouti-coded MIMO-OFDM with superheterodyne structures, the enhanced Alamouti-coded MIMO self-het OFDM has approximately 7.4 dB performance loss at BER of 10^{-3}. The performance loss is due to the fact that approximately half of transmitted power is spent for the transmission of the RF carrier, and a 50% rate loss is required to enable the nonlinear detection. Nevertheless, we remark that MIMO self-het OFDM has the advantage of using an extremely low complexity RF front end, as well as phase noise immunity, which is not available in conventional OFDM with superheterodyne structures.

Fig. 4 compares the BER performance of a standard 2×2 MIMO self-het OFDM and the enhanced 2×2 MIMO self-het OFDM. In this simulation, we assume no phase noise at the receiver, and both systems are encoded by the Golden code. We see that the enhanced scheme provides 2.5 and 3.3 dB gains at BER of 10^{-3} for $P = 2$ and $P = 4$ compared with the standard one, respectively. A diversity gain similar to that of the Alamouti code (from 2 to 3) is observed when using the Golden code. We note that the coded enhanced scheme is approximately 9.7 dB worse than MIMO-OFDM with superheterodyne structures at BER of 10^{-3} [18].

Fig. 5 compares the BER performance of Alamouti-coded MIMO self-het OFDM with SCP ($P = 4$) and Alamouti-coded MIMO-OFDM with superheterodyne in the presence of phase noise. Here, we adopted the OFDM phase noise model used in [31] to simulate the phase noise at the receiver only. We ignore the phase noise generated at the transmitter since it is comparatively insignificant compared with the receiver phase noise and common for both OFDMs. The level of oscillator instabilities is measured by the phase noise linewidth β, and the simulation results are presented for $N\beta/R = 0$ (no phase noise), 0.05, and 0.1, where $R = 2.133 \times 10^7$ is the sampling rate. We see that, for example, when $N\beta/R = 0.1$, we have $\beta \approx 8$ kHz. This demonstrates that, when the phase noise linewidth β is about 0.8% of the OFDM subcarrier spacing $\triangle f = 1$ MHz, the conventional OFDM with superheterodyne structure experiences error floor due to the loss of orthogonality among the subcarriers. For 60 GHz, it was pointed out in [32] that, assuming the same reference oscillator, 60-GHz signals suffer from phase noise that is ten times greater when compared with unlicensed wireless systems below 6 GHz. This indicates that, for 60 GHz, using the same OFDM system as the above, the phase noise linewidth β is about 8% of the OFDM subcarrier spacing and the conventional OFDM experiences an even higher error floor, as shown in Fig. 5.

As shown in Fig. 5, for the Alamouti-coded MIMO-OFDM with superheterodyne receiver structures, an error floor occurs depending on the level of oscillator instabilities at the receiver. Hence, our scheme using SCP outperforms the Alamouti-coded MIMO-OFDM with superheterodyne structures at high SNRs.

Similar behavior is observed for the Golden-coded MIMO self-het OFDM (see Fig. 6). Compared with the Alamouti code, the Golden code is more sensitive to the phase noise, and the error floor occurs at lower SNRs. Hence, Golden-coded MIMO self-het OFDM outperforms the conventional MIMO-OFDM at practical SNR ranges (e.g., at SNR = 15 dB when $N\beta/R = 0.1$ and $N\beta/R = 0.1$).

Finally, we simulate our Alamouti- and Golden-coded self-het OFDM with SCP ($\mathrm{P} = 4$) and conventional MIMO-OFDM in Figs. 7 and 8, respectively, using the parameters from the IEEE *802.11ad* standard [35]–[37]. In both figures, we adopt rate-1/2 low-density parity-check (LDPC) as an outer code with parity check matrix given in [37] and phase noise model in [36], i.e., the phase noise linewidth relative to subcarrier spacing is 0.3 ($\beta N/R = 0.3$). We use $N = 512$, $N_s = N_g = 256, 25\%$ CP, $T_s = 46$ ns, and 50 iterations of LDPC decoding. We adopt QPSK and BPSK signaling for self-het OFDM and conventional OFDM, respectively, to guarantee the same spectral

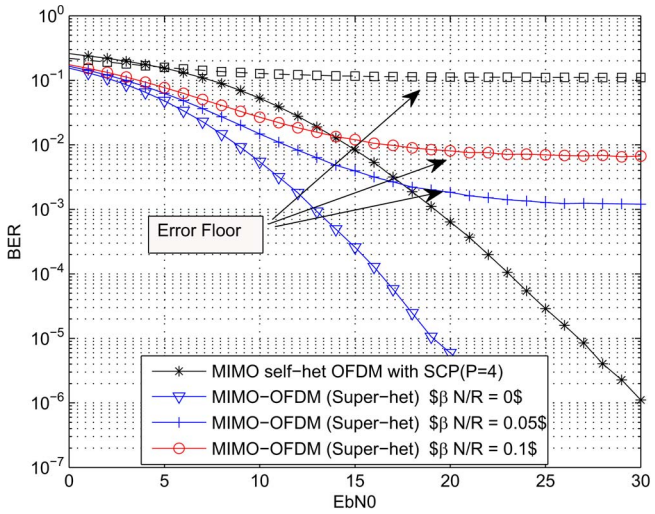

Fig. 6. BER performance comparison of Golden-coded MIMO self-het OFDM with SCP ($P = 4$) and Golden-coded MIMO-OFDM with superheterodyne in the presence of phase noise ($R = 2.133 \times 10^7$).

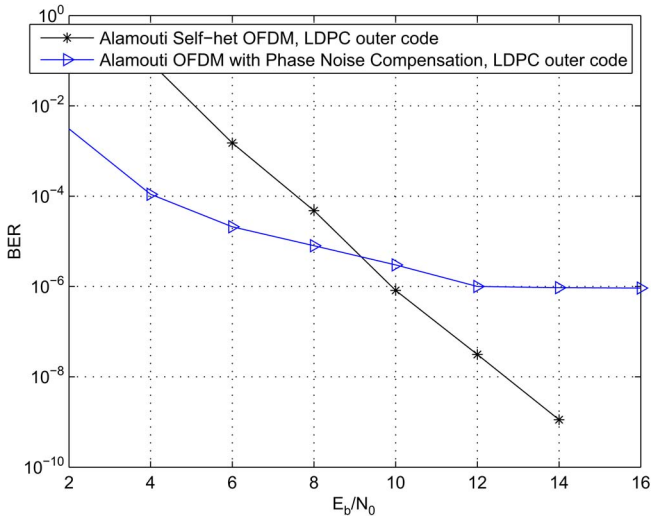

Fig. 7. BER performance comparison of Alamouti-coded enhanced MIMO self-het OFDM with SCP ($P = 4$) and Alamouti-coded MIMO-OFDM with common phase noise compensation, phase noise level ($\beta N/R = 0.3$), and rate-1/2 LDPC as an outer code for both schemes.

efficiency. We observe that, although the channel code lowers the error floor of the conventional OFDM, the self-het OFDM BER will cross over and will not present any flooring effect.

VI. Conclusion

In this paper, we have considered Alamouti- and Golden-coded 2×2 MIMO self-het OFDM with a simple nonlinear detection at the receive antennas. For the Alamouti code, we analytically proved that there is a diversity loss, which can be compensated by the proposed SCP technique. We then showed, by simulations, that the SCP technique improves the BER performance of 2×2 MIMO self-het OFDM with Alamouti and Golden codes by 3.5 and 3.3 dB at BER of 10^{-3}, respectively. We also showed that the proposed SCP STBC MIMO self-het OFDM outperforms the conventional scheme with superheterodyne receivers at high SNRs in the presence of phase noise.

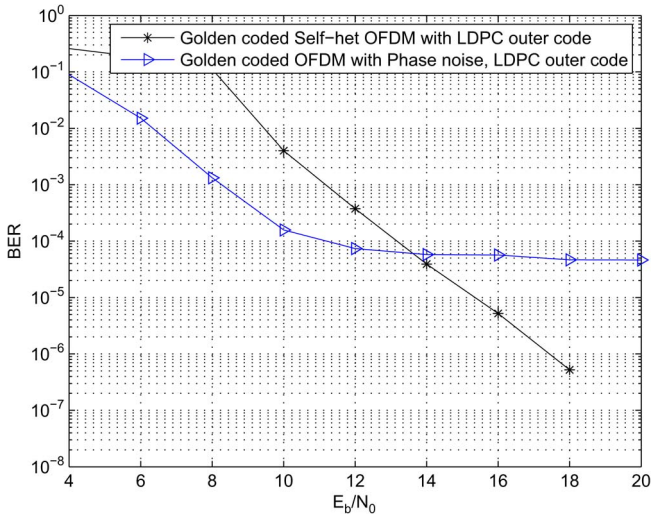

Fig. 8. BER performance comparison of Golden-coded enhanced MIMO self-het OFDM with SCP ($P = 4$) and Golden-coded MIMO-OFDM with common phase noise compensation, phase noise level ($\beta N/R = 0.3$), and rate 1/2 LDPC as an outer code for both schemes.

Finally, we conclude that the phase noise immunity is essential for OFDM systems with small subcarrier spacing, which are heavily degraded by large phase noise found in millimeter-wave receivers.

Appendix A
Proof of Proposition 1

Consider a 2×2 MIMO self-het OFDM using an Alamouti code over MIMO fading channels. From the equivalent model in (10), we obtain

$$\mathbf{H}_{\text{eq}}^H \hat{\mathbf{Y}} = \mathbf{H}_{\text{eq}}^H \mathbf{H}_{\text{eq}} \mathbf{S} + \mathbf{H}_{\text{eq}}^H \hat{\mathbf{Z}} = \Lambda \mathbf{S} + \mathbf{H}_{\text{eq}}^H \hat{\mathbf{Z}} \tag{18}$$

where Λ is given in (12). Let $\tilde{\mathbf{Z}} \triangleq \mathbf{H}_{\text{eq}}^H \hat{\mathbf{Z}} = [\tilde{Z}_1, \tilde{Z}_2]^T$ and $\mathbf{S} = [S_1, S_2]^T$. Without loss of generality, the instantaneous SINR γ associated with S_1, from (18), is given by

$$\gamma = \frac{|\Lambda S_1|^2}{E\left(|\tilde{Z}_1|^2\right)} = \Lambda \frac{E_s}{\sigma_{\tilde{Z}_1}^2} = \Lambda \bar{\gamma} \tag{19}$$

where $\sigma_{\tilde{Z}_1}^2$ is given by (8), and $\bar{\gamma} = E_s/\sigma_{\tilde{Z}_1}^2$ is the average SINR in the kth OFDM subcarrier. For QPSK signaling, the error probability at the kth OFDM subcarrier is given by

$$P_e(k) = \int_0^\infty Q\left(\sqrt{x\bar{\gamma}}\right) f_\Lambda(x)\, dx. \tag{20}$$

Since there is no simple analytical expression for $f_\Lambda(x)$, it is difficult to determine (20). To evaluate the asymptotic behavior of $P_e(k)$, we use the fact that the diversity order of a fading channel is determined by the behavior of $f_\Lambda(x)$ around zero [33]. This is equivalent to the asymptotic behavior of the Laplace transform of $f_\Lambda(x)$ at infinity [33], i.e., if

$$\lim_{s \to \infty} \mathcal{L}\left(f_\Lambda\right) = b s^{-d} + O\left(s^{-(d+\epsilon)}\right) \tag{21}$$

then the diversity order is d for some positive constants b and ϵ.

Let $\nu_1 \triangleq \sum_{m=1}^{2} |H_{1m}|^2$, $\nu_2 \triangleq \sum_{m=1}^{2} |H_{2,m}|^2$, $\hat{\alpha} \triangleq |\alpha_c|^2$, and $\hat{\beta} \triangleq |\beta_c|^2$. Since α_c and β_c are complex Gaussian random variables, both $\hat{\alpha}$ and $\hat{\beta}$ follow an exponential distribution, i.e., $\sim \exp(1/2)$. Since $|H_{rm}|^2 \sim \exp(1)$, then $\nu_1, \nu_2 \sim$ Erlang$(2,1)$. The random variables ν_1 and $\hat{\alpha}$ are independent since the RF carrier and the kth OFDM subcarrier are separated by a minimum of B_g. The cumulative distribution function (cdf) of Λ_1 in (12) then can be written as

$$\begin{aligned} F_{\Lambda_1}(x) &= \int_0^{\infty}\int_0^{\frac{x}{\hat{\alpha}}} \frac{\nu_1}{2} \exp(-\nu_1) \exp\left(-\frac{1}{2}\hat{\alpha}\right) d\nu_1\, d\hat{\alpha} \\ &= 1 - xK_2(\sqrt{2x}) \end{aligned} \tag{22}$$

where $K_v(\cdot)$ denotes the vth order of the modified Bessel function of second kind. Then, the probability density function (pdf) of x can be written as

$$\begin{aligned} f_{\Lambda_1}(x) &= \frac{d}{dx} F_{\Lambda_1}(x) \\ &= -K_2(\sqrt{2x}) + \frac{\sqrt{2x}}{4}\Big(K_1(\sqrt{2x}) + K_3(\sqrt{2x})\Big). \end{aligned} \tag{23}$$

Using the recursive property of the modified Bessel functions (i.e., $zK_{v-1}(z) - zK_{v+1}(z) = -2vK_v(z)$) [34], $f_{\Lambda_1}(x)$ can be further simplified to

$$f_{\Lambda_1}(x) = \frac{\sqrt{2x}}{2} K_1(\sqrt{2x}). \tag{24}$$

The Laplace transform of $f_{\Lambda_1}(x)$ is given by

$$\mathcal{L}\left(f_{\Lambda_1}\right)(s) = \frac{2s + \mathrm{e}^{\frac{1}{2s}} \mathbb{E}\mathrm{i}\left(-\frac{1}{2s}\right)}{4s^2} \tag{25}$$

where $\mathbb{E}\mathrm{i}(\cdot)$ is the exponential integral, and it is defined as $\mathbb{E}\mathrm{i}(z) \triangleq -\int_z^{\infty} \exp(-t)/t\, dt$. Similar expression to (25) can be derived for $f_{\Lambda_2}(x)$.

Since Λ_1 and Λ_2 are independent, the Laplace transform of the pdf of Λ, i.e., $\mathcal{L}(f_\Lambda)(s)$, is given by the product of the individual Laplace transforms, i.e.,

$$\begin{aligned} \mathcal{L}(f_\Lambda)(s) &= f_{\Lambda_1}(s) \times f_{\Lambda_2}(s) \\ &= \frac{1}{4s^2} + \frac{\mathrm{e}^{\frac{1}{2s}} \mathbb{E}\mathrm{i}\left(-\frac{1}{2s}\right)}{4s^3} + \frac{\mathrm{e}^{\frac{1}{s}} \mathbb{E}\mathrm{i}\left(-\frac{1}{2s}\right)^2}{16s^4} \\ &= \frac{1}{4} s^{-2} + \mathrm{O}\left(s^{-(2+\epsilon^+)}\right). \end{aligned} \tag{26}$$

Using the property in (21), we find that the diversity order is 2. ■

Appendix B
Proof of Proposition 2

Considering an Alamouti code is used in this system, we maximize the received RF carrier power at a single receive antenna, i.e., maximizing $|\alpha_c|^2$ only. Then, the RF carrier is positioned such that $l^* = \arg\max_{l \in 1,N} \{|\alpha_c^{(l)}|^2\}$ and l^* is the new RF carrier location. This gives the lower bound of the achievable diversity improvement using the SCP technique.

Let $\hat{\alpha}_1 \triangleq |\alpha_c^{(1)}|^2$, $\hat{\alpha}_N \triangleq |\alpha_c^{(N)}|^2$, $\hat{\alpha} \triangleq |\alpha_c^{(l^*)}|^2$, and $\nu_1 \triangleq \sum_{m=1}^{2} |H_{1m}^{(k)}|^2$. Since the first and the Nth OFDM subcarriers are located apart, it is reasonable to assume that those channels undergo independent fading. Hence, the cdf of $\hat{\alpha}$ is given as

$$F_{\hat{\alpha}}(x) = F_{\hat{\alpha}_1}(x) \times F_{\hat{\alpha}_N}(x) = \left\{1 - \mathrm{e}^{(-x/2)}\right\}^2$$

and the pdf is given as

$$f_{\hat{\alpha}}(x) = \frac{d}{dx}\left\{F_{\hat{\alpha}}(x)\right\} = \mathrm{e}^{(-x/2)}\left\{1 - \mathrm{e}^{(-x/2)}\right\}.$$

We note that the distribution of ν_1 remains unchanged (i.e., $\nu_1 \sim$ Erlang$(2,1)$). Hence, similar to Appendix A, the pdf of Λ_1 is given by

$$f_{\Lambda_1}(x) = \sqrt{2x} K_1(\sqrt{2x}) - 2\sqrt{x} K_1(2\sqrt{x}) \tag{27}$$

and its Laplace transform is given by

$$\mathcal{L}\left(f_{\Lambda_1}\right)(s) = \frac{\mathrm{e}^{\frac{1}{2s}} \mathbb{E}\mathrm{i}\left(-\frac{1}{2s}\right) - 2\mathrm{e}^{\frac{1}{s}} \mathbb{E}\mathrm{i}\left(-\frac{1}{s}\right)}{2s^2}. \tag{28}$$

Although the distribution Λ_1 is altered, the distribution of Λ_2 remains unchanged, and its Laplace transform can be computed similarly to (25). Then, the Laplace transform of $f_\Lambda(x)$ can be written as

$$\begin{aligned} \mathcal{L}\left(f_\Lambda\right)(s) &= \frac{\mathrm{e}^{\frac{1}{2s}} \mathbb{E}\mathrm{i}\left(-\frac{1}{2s}\right)}{4s^3} - \frac{\mathrm{e}^{\frac{1}{s}} \mathbb{E}\mathrm{i}\left(-\frac{1}{s}\right)}{2s^3} \\ &\quad - \frac{\mathrm{e}^{\frac{3}{2s}} \mathbb{E}\mathrm{i}\left(-\frac{1}{s}\right) \mathbb{E}\mathrm{i}\left(-\frac{1}{2s}\right)}{4s^4} + \frac{\mathrm{e}^{\frac{1}{s}} \mathbb{E}\mathrm{i}\left(-\frac{1}{2s}\right)^2}{8s^4} \end{aligned} \tag{29}$$

since Λ_1 and Λ_2 are independent. As $s \to \infty$, $\mathcal{L}(f_\Lambda)(s)$ can be expanded as

$$\lim_{s\to\infty} \mathcal{L}\left(f_\Lambda\right)(s) = \frac{\zeta + \log\left(\frac{2}{s}\right)}{4s^3} + \mathrm{O}\left(s^{-(3+\epsilon)}\right) \tag{30}$$

where ζ is the Euler–Mascheroni constant, and $\epsilon > 0$. Using (21), we see that the lower bound on the diversity order is 3. ■

Appendix C
Proof of Proposition 3

Using an Alamouti code for enhanced 2×2 MIMO self-het OFDM, we maximize the received RF carrier power for both receive antennas independently, i.e., maximize both $|\alpha_c|^2$ and $|\beta_c|^2$ separately. Since the RF carrier locations at both transmitter antennas should be the same, this maximization is impossible. Instead, we analyze the upper bound of the diversity order using the SCP technique. In this case, the pdf's of both Λ_1 and Λ_2 are given in (27). Hence, the Laplace transform of $f_\Lambda(x)$ for this particular case can be written as

$$\begin{aligned} \mathcal{L}\left(f_\Lambda\right)(s) &= f_{\Lambda_1}(s) \times f_{\Lambda_2}(s) \\ &= \frac{\left(\mathrm{e}^{\frac{1}{2s}} \mathbb{E}\mathrm{i}\left(-\frac{1}{2s}\right) - 2\mathrm{e}^{\frac{1}{s}} \mathbb{E}\mathrm{i}\left(-\frac{1}{s}\right)\right)^2}{4s^4}. \end{aligned} \tag{31}$$

As $s \to \infty$, $\mathcal{L}(f_\Lambda)(s)$ can be expanded as

$$\lim_{s\to\infty} \mathcal{L}(f_\Lambda)(s) \approx \frac{\left(\zeta + \log(2)\right)^2}{4s^4} + \mathrm{O}\left(s^{-(4+\epsilon^+)}\right). \tag{32}$$

Using (21), the upper bound on the diversity order is 4. ■

ACKNOWLEDGMENT

This work was performed at the Monash Software Defined Telecommunications Laboratory.

REFERENCES

[1] P. Smulders, "Exploiting the 60 GHz band for local wireless multimedia access: Prospects and future directions," *IEEE Commun. Mag.*, vol. 40, no. 1, pp. 140–147, Jan. 2002.

[2] H.-J. Song and T. Nagatsuma, "Present and future of terahertz communications," *IEEE Trans. Terahertz Sci. Technol.*, vol. 1, no. 1, pp. 256–263, Sep. 2011.

[3] Y. Shoji, M. Nagatsuka, K. Hamaguchi, and H. Ogawa, "60 GHz band 64 QAM/OFDM terrestrial digital broadcasting signal transmission by using millimeter-wave self-heterodyne system," *IEEE Trans. Broadcast.*, vol. 47, no. 3, pp. 218–227, Sep. 2001.

[4] T. Nagatsuma, "Generating millimeter and terahertz waves," *IEEE Microw. Mag.*, vol. 10, no. 4, pp. 64–74, Jun. 2009.

[5] K. Ono, T. Saito, N. Hidaka, Y. Ohashi, and Y. Aoki, "A 60-GHz HEMT-based MMIC direct-detection receiver for application in non-contact ID card systems," *Proc. 25th Eur. Microw. Conf.*, Sep. 1995, vol. 2, pp. 996–1000.

[6] J. N. Schulman *et al.*, "W-band direct detection circuit performance with Sb-heterostructure diodes," *IEEE Microw. Wireless Compon. Lett.*, vol. 14, no. 7, pp. 316–318, Jul. 2004

[7] Y. Shoji, K. Hamaguchi, and H. Ogawa, "Millimeter-wave remote self-heterodyne system for extremely stable and low-cost broad-band signal transmission," *IEEE Trans. Microw. Theory Tech.*, vol. 50, no. 6, pp. 1458–1468, Jun. 2002.

[8] Y. Shoji and H. Ogawa, "70-GHz-band MMIC transceiver with integrated antenna diversity system: Application of receiver-module-arrayed self-heterodyne technique," *IEEE Trans. Microw. Theory Tech.*, vol. 52, no. 11, pp. 2541–2549, Nov. 2004

[9] C. Choi and Y. Shoji, "Third-order intermodulation distortion characteristics of millimeter-wave self-heterodyne transmission techniques," in *Proc. APMC*, Dec. 2006, pp. 1751–1756.

[10] Y. Shoji and H. Ogawa, "High-receiving-sensitivity 70-GHz band MMIC transceiver: Application of receiving-module-arrayed self-heterodyne technique," in *Proc. IEEE MTT-S Int. Microw. Symp.*, Jun. 2004, vol. 1, pp. 219–222.

[11] C. Choi, Y. Shoji, and H. Ogawa, "Analysis of receiver space diversity gain for millimeter-wave self-heterodyne transmission techniques under two-path channel environments," in *Proc. IEEE Radio Wireless Symp.*, Jan. 2007, pp. 75–78.

[12] Y. Shoji, C. Choi, and H. Ogawa, "Millimeter-wave OFDM WPAN system applying adaptive modulation for grouped sub-carriers," in *Proc. IEEE Radio Wireless Symp.*, Jan. 2007, pp. 499–502.

[13] C. Choi, Y. Shoji, and H. Ogawa, "Implementation of an OFDM baseband with adaptive modulations to grouped subcarriers for millimeter-wave wireless indoor networks," *IEEE Trans. Consum. Electron.*, vol. 57, no. 4, pp. 1541–1549, Nov. 2011.

[14] Y. Haibing, P. F. M. Smulders, and M. H. A. J. Herben, "Frequency selectivity of 60-GHz LOS and NLOS indoor radio channels," in *Proc. IEEE VTC Spring*, May 2006, pp. 2727–2731.

[15] P. Smulders, "Statistical characterization of 60-GHz indoor radio channels," *IEEE Trans. Antennas Propag.*, vol. 57, no. 10, pp. 2820–2829, Oct. 2009

[16] X. Hao, V. Kukshya, and T. S. Rappaport, "Spatial and temporal characteristics of 60-GHz indoor channels," *IEEE J. Sel. Areas Commun.*, vol. 20, no. 3, pp. 620–630, Apr. 2002.

[17] Y. Azar, G. N. Wong, and T. S. Rappaport, "28 GHz propagation measurement or outdoor cellular communication using steerable beam antenna," in *Proc. IEEE ICC*, Budapest, Hungary, Jun. 2013, pp. 5143–5147.

[18] N. Fernando, Y. Hong, and E. Viterbo, "Self-heterodyne OFDM transmission for frequency selective channels," *IEEE Trans. Commun.*, vol. 61, no. 5, pp. 1936–1946, May 2013.

[19] N. Fernando, Y. Hong, and E. Viterbo, "Subcarrier pairing for self-heterodyne OFDM," in *Proc. IEEE ICC*, Budapest, Hungary, Jun. 2013, pp. 3105–3109.

[20] H. Zhang, S. Venkateswaran, and U. Madhow, "Channel modeling and MIMO capacity for outdoor millimeter wave links," in *Proc. IEEE Wireless Commun. Netw. Conf.*, Sydney, N.S.W., Australia, Apr. 2010, pp. 1–6.

[21] E. Torkildson, H. Zhang, and U. Madhow, "Channel modeling for millimeter wave MIMO," in *Proc. ITA Workshop*, San Diego, CA, USA, Feb. 2010, pp. 1–8.

[22] H. Bolcskei and A. J. Paulraj, "Space–frequency coded broadband OFDM systems," in *Proc. IEEE Wireless Commun. Netw. Conf.*, Chicago, IL, USA, Sep. 2000, pp. 1–6.

[23] S. Alamouti, "A simple transmit diversity technique for wireless communications," *IEEE J. Sel. Areas Commun.*, vol. 16, no. 8, pp. 1451–1458, Oct. 1998.

[24] P. Xia, S. Zhou, and G. B. Giannakis, "Adaptive MIMO-OFDM based on partial channel state information," *IEEE Trans. Signal Process.*, vol. 52, no. 1, pp. 202–213, Jan. 2004

[25] J. C. Belfiore, G. Rekaya, and E. Viterbo, "The Golden code: A 2×2 full-rate space–time code with nonvanishing determinants," *IEEE Trans. Inf. Theory*, vol. 51, no. 4, pp. 1432–1436, Apr. 2005.

[26] L. Zheng and D. N. C. Tse, "Diversity and multiplexing: A fundamental tradeoff in multiple-antenna channels," *IEEE Trans. Inf. Theory*, vol. 49, no. 5, pp. 1073–1096, May 2003.

[27] E. Viterbo and J. Boutros, "A universal lattice code decoder for fading channels," *IEEE Trans. Inf. Theory*, vol. 45, no. 5, pp. 1639–1642, Jul. 1999.

[28] V. Tarokh, N. Seshadri, and A. R. Calderbank, "Space–time codes for high data rate wireless communication: Performance criterion and code construction," *IEEE Trans. Inf. Theory*, vol. 44, no. 2, pp. 744–765, Mar. 1998.

[29] O. Tirkkonen and A. Hottinen, "Square-matrix embeddable space–time block codes for complex signal constellations," *IEEE Trans. Inf. Theory*, vol. 48, no. 2, pp. 384–395, Feb. 2002.

[30] E. Biglieri, Y. Hong, and E. Viterbo, "On fast-decodable space–time block codes," *IEEE Trans. Inf. Theory*, vol. 55, no. 2, pp. 524–530, Feb. 2009.

[31] S. Wu and Y. Bar-Ness, "OFDM systems in the presence of phase noise: Consequences and solutions," *IEEE Trans. Commun.*, vol. 52, no. 11, pp. 1988–1996, Nov. 2004.

[32] R. C. Daniels and R. W. Heath, "60 GHz wireless communications: Emerging requirements and design recommendations," *IEEE Veh. Technol. Mag.*, vol. 2, no. 3, pp. 41–50, Sep. 2007.

[33] W. Zhengdao and G. B. Giannakis, "A simple and general parameterization quantifying performance in fading channels," *IEEE Trans. Commun.*, vol. 51, no. 8, pp. 1389–1398, Aug. 2003.

[34] I. S. Gradshteyn, I. M. Ryzhik, A. Jeffrey, and D. Zwillinger, *Table of Integrals, Series, and Products*, 6th ed. San Diego, CA, USA: Academic, 2000.

[35] *Wireless LAN at 60 GHz—IEEE 802.11ad Explained, Application Note*, Agilent Technol., Santa Clara, CA, USA, 2013.

[36] *TGad Evaluation Methodology*, IEEE 802.11-09/0296r16, 2010.

[37] S. Skotnikov, "Low power LDPC decoder design for 802.11ad standard," M.S. thesis, Univ. California, Berkeley, CA, USA, 2012.

Nirmal Fernando received the B.Sc.(Hons.) and PG.Dip. degrees from the University of Moratuwa, Moratuwa, Sri Lanka, in 2006 and 2009, respectively, and the Ph.D. degree from Monash University, Clayton, Australia, in 2014.

He is currently a Project Technical Leader with Airservices Australia, Brisbane, Australia. He was a Lecturer with the University of Moratuwa from 2009 to 2010 and an Engineer at Dialog Telekom, Colombo, Sri Lanka, from 2006 to 2009. His research interests include noncoherent orthogonal frequency-division multiplexing (OFDM) techniques, low-complexity radio-frequency receivers, optical OFDM, multiple-input–multiple-output precoding, signal processing in wireless communications, and communication theory.

Yi Hong (M'00–SM'10) received the Ph.D. degree in electrical engineering and telecommunications from the University of New South Wales (UNSW), Sydney, Australia, in 2004.

She has been with the Institute for Telecommunications Research, University of South Australia, Adelaide, Australia; the Institute of Advanced Telecommunications, Swansea University, Swansea, U.K.; and the University of Calabria, Rende, Italy. She is currently a Senior Lecturer with the Department of Electrical and Computer Systems Engineering, Monash University, Clayton, Australia. Her research interests include information and communication theory with applications to telecommunications engineering.

Dr. Hong is a Technical Program Committee Member for many IEEE conferences, such as the IEEE International Conference on Communications; Vehicular Technology Conference; International Symposium on Personal, Indoor, and Mobile Radio Communications; and the Wireless Communication and Networking Conference. She was the Publicity Chair of the 2009 IEEE Information Theory Workshop, Sicily, Italy. She was the Technical Program Committee Chair of the 2011 Australian Communications Theory Workshop, Melbourne, Australia; and the General Co-Chair of the 2014 IEEE Information Theory Workshop, Hobart, Australia. She is an Associate Editor of the *European Transactions on Telecommunications*. During her Ph.D. studies, she received an International Postgraduate Research Scholarship from the Commonwealth of Australia; a Supplementary Engineering Award from the School of Electrical Engineering and Telecommunications, UNSW; and a Wireless Data Communication System Scholarship from UNSW. She also received the NICTA-ACoRN Earlier Career Researcher Award for a paper presented at the Australian Communication Theory Workshop (AUSCTW), Adelaide, Australia, 2007.

Emanuele Viterbo (M'95–SM'04–F'11) was born in Torino, Italy, in 1966. He received the Laurea and Ph.D. degrees in electrical engineering from the Politecnico di Torino, Torino, in 1989 and 1995, respectively.

From 1990 to 1992, he was with the European Patent Office, The Hague, The Netherlands, as a Patent Examiner in the field of dynamic recording and error-control coding. Between 1995 and 1997, he held a postdoctoral position with the Dipartimento di Elettronica, Politecnico di Torino, on communications techniques over fading channels. He became an Associate Professor with the Dipartimento di Elettronica, Politecnico di Torino, in 2005 and a Full Professor with the Dipartimento di Elettronica Informatica e Sistemistica, Università della Calabria, Rende, Italy, in 2006. Since 2010, he has been a Full Professor with the Department of Electrical and Computer Systems Engineering, Monash University, Clayton, Australia, and the Associate Dean Research Training of the Faculty of Engineering at Monash. In 1993, he was a Visiting Researcher with the Communications Department, German Aerospace Center (DLR), Oberpfaffenhofen, Germany. In 1994 and 1995, he was visiting the E.N.S.T., Paris, France. In 1998, he was a Visiting Researcher with the Information Sciences Research Center, AT&T Research, Florham Park, NJ, USA. In 2003, he was a Visiting Researcher with the Mathematics Department, Swiss Federal Institute of Technology Lausanne (EPFL), Lausanne, Switzerland. In 2004, he was a Visiting Researcher with the Telecommunications Department, University of Campinas, Campinas, Brazil. In 2005, he was a Visiting Researcher with the Institute for Telecommunications Research, University of South Australia, Adelaide, Australia. His main research interests are in lattice codes for Gaussian and fading channels, algebraic coding theory, algebraic space–time coding, digital terrestrial television broadcasting, and digital magnetic recording.

Dr. Viterbo was an Associate Editor of the IEEE TRANSACTIONS ON INFORMATION THEORY, the *European Transactions on Telecommunications*, and the *Journal of Communications and Networks*. He is now an Editor of *Foundations and Trends in Communications and Information Theory*. He received a NATO Advanced Fellowship in 1997 from the Italian National Research Council.